

UAH NO: 5-32274
CONTRACT NO: NAS8-36955 D.O.54

PREPARED BY Y. TAKAHASHI



FINAL REPORT

**DEVELOPMENT OF A SCINTILLATING OPTICAL FIBER
IONIZATION CALORIMETER**

**Cosmic Ray Laboratory
College of Science
The University of Alabama in Huntsville
Huntsville, AL35899
TEL: 205 - 895 - 6028/6259**

October 1, 1990

(NASA-CR-184415) DEVELOPMENT OF A
SCINTILLATING OPTICAL FIBER
IONIZATION CALORIMETER Final Report
(Alabama Univ.) 35 p

N93-11662

Unclas

G3/35 0127410

488625

CONTENTS

1. INTRODUCTION AND OVERVIEW
2. DESIGN REQUIREMENTS
 - 2-1 Size and Weight of the SOFIC
 - 2-2 Three-Dimensional Segmentation of the SOFIC
3. DESIGN OF A CALORIMETER
 - 3-1 Scintillation Fiber
 - 3-2 Lead Plates
 - 3-3 Fiber - Lead Alignment and Bonding
4. DESIGN OF READ-OUT SYSTEM
 - 4-1 Multi-Channel-Plate Image Intensifier
 - 4-2 Multi-Anode Photo-Counting Tubes
 - 4-3 Charge-Coupling-Device (CCD Camera)
 - 4-4 Data Acquisition
5. EXPECTED PERFORMANCE OF A CALORIMETER FOR HIGH ENERGY NUCLEI AND GAMMA-RAYS
6. SUMMARY
7. REFERENCES

1. INTRODUCTION AND OVERVIEW

Calorimeters to measure energies of high energy photons and hadronic particles have been used in both nuclear physics and astrophysics experiments for more than three decades. High energy particles, in their passage through dense matter form electron-photon cascades. Very high energies, such as 1 TeV (1 trillion electron volts) or more found in cosmic rays cannot be measured directly unless the total energy is segmented into lower energy particles.

The primary particle, be it photon or nucleus, forms a cascade of low-energy electrons and photons by both electro-magnetic and hadronic interactions in dense matter. The total energy measurements of these electron-photon cascade showers allow an estimate of the energy of the primary incoming particle. A calorimeter typically consists of lead plates and scintillators which record the light yield of the cascade.

As a cascade shower detector, plastic scintillators have two main advantages:

- the light signal is proportional to the energy deposition
- fast detection of deposited energy when coupled with photomultipliers; the FWHM of the signal is of a few nanoseconds with a time resolution of 150 picosecond.

Nevertheless, they are usually poor in localizing ability (unable to give spatial resolution to better than several centimeters). Because of this weakpoint, scintillator calorimeters could not utilize three-dimensional shower theory. Three dimensional cascade theory was very well established by 1955, which permitted, in principle, sampling calorimetry within a small radius, without measuring the total absorption energy in a large volume.

Conventional calorimeters had to utilize one-dimensional cascade theory in energy measurement, as they cannot detect the lateral profile of a cascade. Consequently, a scintillator calorimetry is required to measure a total light yield in matter whose depth must be semi-infinite. This makes a calorimeter extremely large and heavy, yet its geometrical aperture is very much limited to such as 0.1 steradian or less. For measuring high energy particles, more than 100 tons of the equipment is needed for a calorimeter, which has practically precluded the use of these calorimeters in space.

Scintillation fiber technology developed in the last decade has significantly improved the spatial resolution of a calorimeter, promising a realistic utilization of three-dimensional calorimetry.

The tasks of the contract NAS8-36955 D.O. 54 was to further the design for the development of "A Scintillating Fiber Ionization Calorimeter" (SOFIC), as listed below. The design study is focused on a SOFIC capable of tracking and energy measurements of cosmic ray particles from protons to iron and of gamma rays in the energy region 1 TeV and above.

1. Initiate a study of the transmission efficiency of commercially available scintillating fibers (GFE) over at least their characteristic absorption length.
2. Estimate the variation of practically-achievable light collection efficiency with available fibers at lengths characteristic of a SOFIC (0-2 meters).
3. Consider and evaluate several proposed designs of SOFIC in terms of stack design, detection readout and data-handling.
4. Consider optical matching between the fiber bundles and the electro-optical detection device.

This report describes performed studies. The design requirements for the SOFIC is summarized in Section Two. Section Three describes the designs of a calorimeter in consideration. The design characteristics include geometry and sequence of fiber alignment. Reported in Section Four is the read-out system, which has two options for the device, namely, multi-anode phototube or CCD camera. The data acquisition is described in Section Five.

FINIS

2. DESIGN REQUIREMENTS

The SOFIC is a calorimeter used to measure cascade showers with energy above 1 TeV. It must be reasonably light so as to be flown on available stratospheric balloons. Considering the low intensity of high energy cosmic rays, the geometrical factor must be maximized within a limited payload weight. The first boundary condition for a design is therefore a weight limit and the size of the calorimeter. The thickness of the detector should be larger than the length of the shower maximum within a radius of 1 Moliere unit (~ 5 mm).

The structural design of a calorimeter depends on the demand of segmentation in both longitudinal and radial sampling. The horizontal segmentation of a calorimeter (x- and y-axes) should be made in such a way that individual pixel size should be smaller than 10% of the 1 Moliere Length (M.L.); otherwise, radial information would not be retrieved.

2-1 Size and Weight of the SOFIC

The typical payload on balloons is about 1.5 tons including the weight of the gondola and the detector. About 1,200kg is considered reasonable for a detector weight. The area size of the SOFIC depends on the thickness of the lead absorber. Considering a required thickness for measuring energies of nuclei up to 100 TeV/nucleon, the SOFIC must be at least 14 radiation lengths deep, which approximately corresponds to the shower maximum in 1 Moliere length for the highest energy photons (about 10 TeV), in these interactions.

The material density of lead is 11.35 g/cm^3 , and its radiation length (R.L.) is 6.37 g/cm^2 . The 14 R.L. equals to 89.2 g/cm^2 . For a 1,000kg calorimeter, this thickness gives the area size of about $(100 \text{ cm})^2$. An actual instrument would weigh about 30% more including fibers, bonding material, cables, electronics and optics, and batteries. In this study we consider the calorimeter size of $1 \text{ m}^2 \times 14 \text{ R.L.}$ for the purpose of simplicity. The final size can be adjusted to the given payload allowance, by simply reducing the area size accordingly.

2-2 Three Dimensional Segmentation of the SOFIC

A very coarse longitudinal segmentation is often used in most one-dimensional ionization calorimeters. The limitation in number of usable electronic channels for phototube readout in conventional calorimeter has been one of the major reasons. The other reason has been

that finer longitudinal segmentation does not give any more information than the total ionization which a coarse segmentation can provide.

The three-dimensional calorimeter allows observation of detailed shower profile. Showers initiated by photons or hadrons (such as nuclei) can be statistically discriminated by the starting depth of the shower. This discrimination is made possible by the difference in mean free path of these particles. When one can determine the starting depth (t_0) with a resolution about 0.5 radiation or better, more than 95% of gamma-rays can be identified by asking for $(t_0) < 4.0$ R.L., while about 15% of hadrons would mimic gamma-rays. If the (t_0) can be measured to 0.1 R.L., more than 95% of gamma-rays will be found within to < 3.0 R.L., while only 10% of hadrons contaminate the data. This illustrates an advantage of finer longitudinal segmentation in the first few R. L.'s of lead.

If coupled with finer lateral segmentation by 1mm fibers, associated heavy tracks emanating from hadronic interactions can be detected as in Fig. 1. Showers initiated by photons or electrons do not bear any signals of heavy prongs in its entire cascade development. Hadronic showers would show an average of 5 heavy prongs at 100 GeV, the multiplicity of which increases logarithmically with primary energy. Monte Carlo simulation shows that the longitudinal segmentation of about 2mm lead with 1mm horizontal segmentation permits 98% discrimination of photons from hadrons. If coupled with the longitudinal information on (t_0) , 99.9% of photons can be identified while contamination from hadrons is limited to only 0.2%.

From the reasons described above we consider x- and y- fiber arrays at every 2mm thicknesses of lead plates, although the factor of two relaxation in longitudinal segmentation (4mm thick) can still provide similar capability.

The horizontal segmentation is determined by the size of the fiber. The smaller the fiber cross section, the better the lateral resolution. In fact, the latest fiber production technology allows a very small cross section, such as 50 microns. Light yield, however, decreases with decreasing size of a fiber. To maintain an observability of single minimum-ionizing particle and mechanical strength, we consider 1mm x 1mm square cross-section fibers. Smaller fibers, if mechanically stabilized in the future, can be considered for the SOFIC. The other reason to choose a 1mm fiber is due to a desire to read out all fibers in the SOFIC by a single CCD camera (500-1000 lines). Fig. 2 shows a bird's eye view and cross section of the SOFIC.

3. DESIGN OF A CALORIMETER

3-1 Scintillation Fiber (SF)

All types of scintillating fiber possess a scintillating core material surrounded by a non-scintillating optical cladding that provides a highly reflective surface to contain emitted light inside a narrow cone of a critical half angle. Interface between the core and cladding must be optically smooth. The cladding material must be transparent and thicker than the depth of several wavelengths since the electromagnetic wave extends into the cladding.

The cladding also serves to isolate the reflective surface from mechanical or chemical damage. Fibers are flexible and more easily shaped and handled than sheets of scintillator where the reflective surface is bare. However, the macroscopically smooth surface of cladding often suffers microscopic cracks when bent or mechanically twisted. Also, chemical bonding with other material for a long period of time sometimes degrade the surface properties, and lead to an unexpectedly short attenuation length.

A typical sheet of plastic scintillator traps about 10 - 15% of light emitted isotropically along a track in the sheet. The fraction of the total scintillation light trapped in each direction in a fiber can be approximated by $0.5 \times [1 - n'/n_0]$, where n' and n_0 are refractive indices of the cladding and the core, respectively. This value for glass, plastic and liquid SF's are small, namely, between 2.5% - 4% as opposed to 10 - 15% efficiency of sheets. This is partly due to the fiber geometry (small radius leads to a larger ratio of surface area vs. volume for light escape), and partly due to non-meridional rays. Table 1 lists approximate optical trapping efficiencies of commonly used SF's.

MEDIUM	CORE	N_0	CLADDING	N'	EFFICIENCY
Plastic	Polystrene + PND + POPOP	1.59	Polyvinyl acetate	1.46	4.10%
Glass	GSO	1.59	N51A	1.51	2.50%
Liquid	Methyl- naphthalene + bis-MSB	1.62	N51A	1.51	3.40%

The key characteristics of SF include:

- (1) Compact and high density of hits per unit path length. Minimum ionizing particles generate 5 photoelectrons per 1 mm of plastic SF in a PMT at a distance of 1m along the fiber.
- (2) Fine spatial resolution; as good as rms = 20 microns for glass SF.
- (3) Excellent two-track resolution; namely, 50 microns for glass-type SF.
- (4) Absence of signal saturation for singly charged particles up to extremely high particle densities.
- (5) Radiation hardness, withstanding 1 million rads with tolerable losses in light-efficiency.
- (6) Flexible, allowing curved surfaces.
- (7) Fast response; the pulse time within 1 ns and the pulse integration time is < 20 ns.
- (8) Insensitivity to the magnetic fields.

Additional characteristics advantageous for a calorimeter includes:

- (1) High density achievable with pb packing, (R.L. < 1 cm).
- (2) Good hermeticity and uniformity of response with respect to impact position and angle.
- (3) Good energy resolution for electromagnetic showers, due to the fine sampling capability.
- (4) High imaging capability for precise location of the core of the shower.

Utilization of these qualities, however, needs some caution. First of all, the stability of light efficiency and attenuation length must be carefully considered. The pure fiber after production normally exhibits excellent uniformity and long attenuation length. These qualities, however, degrade by bending, bonding, and thermal cyclings. Restricting the radius of curvature of bending will certainly prevent some degradation. A bonding material must be chosen which is chemically inert on the surface of the SF and has a thermal expansion coefficient close to that of the SF.

There are several types of scintillation fibers available on the present market. For example:

- (1) Polystyrene + Wave Length Shifters + Oxygen Quencher with PMMA cladding
- (2) SCSN38
- (3) SCSN81
- (4) Polystyrene + 3HF
- (5) Polystyrene + "PMP"

We have learned directly by lab. examination, and also indirectly from other study groups, that the SF of type N-201 of Kyowa Gas Inc. is known to be most uniform and stable for fabrication purpose. It maintains a high fluorescence (225 mV) while having a long attenuation length (180 cm) after a severe bending with a curvature of about 7 cm bonded with lead strings by epoxy.

In addition to the above described stability, availability of the size and shape constitutes an important factor for the design.

The most common shape is with a round cross section. The round shape SF provides the best mechanical strength of the SF surface and a constancy in light efficiency for different incoming angles. Nevertheless, when combined with heavy metal such as pb for 14 R.L. (90 g/cm**2), the round shape suffers substantial pressure on the top and bottom points, which leads to microcracks of fiber surfaces. Therefore, the square or octagonal cross-section is more advantageous in actual construction of a calorimeter, as long as the cracks during the pulling/draw procedure of the production at the manufacturer is minimized. The type N-201 has been well proven with respect to this problem, and has been used in a number of detectors built at the European Center for Nuclear Research.

3-2 Lead Plates

The main absorber material in a typical calorimeter is lead. Other materials such as uranium and tungsten are sometimes used for specific purposes; i.e., to improve the energy resolution to the order of 5% and 10% at 1 GeV, respectively. Despite their excellent energy resolution (due to a high atomic number or density), the latter metals are hard to handle in manufacturing and are very expensive. For practical reasons, pure lead plates are best suited to accommodate scintillation fibers in between layers of plates. In particular, the sufficiently soft property of pure lead plates helps installation of fibers with minimum damage to their cladding thereby assuring presentation of optical properties and performance close to those obtained in bench-tests of individual fibers.

The nuclear properties of lead plates for high energy calorimetry can be characterized by its radiation length (X_0) and nuclear collision length ($LAMBDA$).

$$X_0 = 6.37 \text{ g/cm}^2 = 0.56 \text{ cm}$$

$$LAMBDA = 116.2 \text{ g/cm}^2 = 10.23 \text{ cm}$$

Lead has a density of 11.35 g/cm³, an atomic number (Z) of 82 and atomic mass number (A) of 207, which theoretically characterize the energy resolution of calorimeter as

$$\Delta E / E = 13 - 16 / \sqrt{(E/\text{GeV})\%}$$

The calorimeter in consideration for high energy cosmic ray experiments will be used in the energy regime exceeding 100 GeV. The lead calorimeter at these energies will give the energy resolution better than 2% at 100 GeV and above. The expected energy resolution based upon the lab. test performed at a high energy accelerator at Tsukuba, Japan, is illustrated in Fig. 3.

In conclusion, the lead provides absorber material of the scintillation fiber calorimeter for high energy cosmic ray experiments with three major practical advantages:

- 1) easiness in handling and manufacturing
- 2) highest cost effectiveness
- 3) sufficient energy resolution

3-3 Fiber-Lead Alignment

The manufacturing process of a SF calorimeter must include accurate alignment of fibers on lead plates. In order to provide sufficient accuracy in the x- and y-coordinates as well as that of the depth (z-coordinate) to locate the electromagnetic cascade showers. The required accuracy is not too demanding relative to its diameter of about 1mm². Alignment to 100 microns will suffice for the application of three dimensional calorimetry.

The electron-photon cascade shower develops with the increasing thickness of the absorber. The number density of electrons increases to some thickness (T_c: shower maximum) and then decreases by absorption. The T_c increases with increasing energy of the cascade, and also with increasing radius measured from the shower axis. This lateral spread of electrons from the center of the shower axis can be well characterized by the Moliere Length (M.L.). The 1 M.L. measures the r.m.s. average of the lateral spread of electrons at the shower maximum. The 1 M.L. in pure lead is 5 mm, while in the SF calorimeter under consideration is about 10mm. The longer M.L. value for the SF calorimeter is due to the geometrical spacing (dilution) factor of about 2.0 (lead + SF / lead) in the suggested design. Thus, the alignment accuracy of 100 microns will provide 1% resolution of the lateral distribution of the cascade, which is practically sufficient to measure the lateral spread of cosmic ray gamma -rays and nuclei events.

The length of individual fibers depends on the calorimeter size. For a SF calorimeter with the area of $1\text{m} \times 1\text{m}$, the required length of an individual fiber depends on its location. At least 50 cm extra length of fibers from each edges of the SF calorimeter is required so that edges of each fibers be collected into a single bundle. The longest lengths from the edges may be 1m , which is for the fibers at the far ends of other edges of the SF calorimeter. Fig. 4 illustrates the geometric variation of required lengths of the fibers. Considering the fact that the fibers must be collected at both edges, 2m - 3m long fibers are required.

Below we describe a scheme to manufacture a SF calorimeter.

1. Assembly of SF Arrays

- a. First, prefabricate SF's. The 1,000 SF's must be glued with epoxy side-by side on a 1m wide board having right-angled vertical supports at edges. Make 80 SF boards (40 for x- and 40 for y-axes).
- b. Next, place-on a table a flat aluminum board that can keep flatness to better than $1/2\text{ mm}$ over 1 m length under uniform load of about 100 g/cm^2 . The $3/4\text{''}$ aluminum honeycomb board is most appropriate for this purpose. All the edges of the board must be reinforced by the solid aluminum blocks so that the board edges stay intact when lifted up or landed with a shock of about 5g . This mechanical design must be revised for the container of the SF calorimeter. Here we confine ourselves to the mechanical strength required for the construction of a SF calorimeter.
- c. Apply epoxy on a honeycomb board and place a SF board (y-axis). Place a flat pressing board over the SF board and apply a small pressure to about 1 PSI . Leave for about 8 hours for epoxy to harden. Remove pressing board, and then, apply epoxy over the top surface of a SF board.
- d. The fabrication cycle starts: the 1 mm thick lead plate should be placed on the above SF board, and rolled over with a heavy metal roller. The work should continue until the surface is as flat as $+0.1\text{ mm}$. Then, epoxy must be applied on the top surface of the lead plate.
- e. Another SF board (x-axis) will be placed, and a board of $1\text{m} \times 1\text{m}$ be applied over the SF to press the SF down into the epoxy that was coated on a lead plate. Then, apply epoxy over the top of the SF board and place another 1mm thick lead plate on it. Roll the lead surface with a heavy metal roller smoothly.
- f. Repeat (4) and (5) for the next y-axis SF board.

- g. Continue the above cycle for x- and y- axes SF boards until the total number of cycles reaches 40 (40 x and 40 y).
- h. On the top of the last lead plate, apply epoxy. Place another honeycomb board over it. Leave-it with weight board on it until it hardens. This honeycomb board becomes the ceiling board of the SF calorimeter.

2. Edge Treatment and Formation of A Bundle

Each fiber must be appropriately bent so as to form a single bundle with other fibers. The mechanical strength of the fiber's clad must be taken into account when bending the fiber. Slow and careful bending to a curvature of about 20cm is relatively easy and safe. Clads of a fiber will undergo micro-cracking when a sudden bending force is applied, or bending with a extremely small curvature is attempted. We tested samples of Kyowa Gas Company SCSN-8IT. The majority of these samples showed negligible cracks at a diameter of 15cm. There are other plastic SF's on the market. Most of them have been used in many accelerator experiments with a bending curvature not exceeding about 30 cm.

The smallest curvature occurs when SFs' are bent at the horizontal edges. A design that minimizes the cracking danger of SFs' is considered in Fig. 5 in which curving is kept with a diameter larger than 30 cm. A prototype made by our colleagues at the National Laboratory for High Energy Physics (Prof. F. Takasaki) used 10cm curvature, and the loss of light due to microcracks was reported as 23%.

3. Installation Into A Supporting Box

A SF calorimeter that minimizes the curving cracks need a large area supportive flat. Fig. 5 shows SF calorimeter whose edges are supported by multiple layers of paper-honey-comb boards. The entire area measures 220 cm x 220 cm. This set can be mounted in a supporting box of the gondola of Fig. 6. The other electronics and telemetry devices with Ni-Ca batteries can be mounted in a box shelf made at the bottom of the supporting box.

The bottom of the entire gondola is going to be equipped with very thick paper honeycomb (60cm - 2 ft) to absorb a landing shock.

4. Design of Read-Out System

There are two options for the read-out system of the optical output: (1) multi-anode photo-counting tubes (PMT), or (2) charge-coupled divide (CCD). The former must be used for accelerator experiments in which the beam intensity is high, and fast timing is required. The latter is a slow device but simple, and is most suitable for cosmic ray observation. The low energy cosmic ray showers require image-intensification, while very high energy showers do not.

4-1 Multi-Channel-Plate Image Intensifier

A multi-channel-plate image intensifier is a significant help for either PMT or CCD readouts, because the raw optical output from low energy showers is too low to be detected sufficiently above the noise level. A multi-channel-plate image intensifier shown in Fig. 7 can multiply the signal by a factor of 3×10^3 . A typical model has two stages of this device, multiplying the initial signal by a factor of 10^7 times.

The quantum efficiency of multi-channel-plate is about 10% at the wavelength of 450 - 550 nm. (Fig. 8) The overall spectral response curve differs from model to model, but they are typically sensitive to 370 - 650 nm. The geometrical magnification is normally 1.0 unless it is coupled to optical lens for CCD camera.

All 40 planes of SF's on one face of the calorimeter are read as one unit. The total number of fibers per face is 1,000 mm x 40mm, which should be formed into a bundle suitable for an interface to multi-channel-plate and CCD readout. Since the multi-channel plate has a circular opening (25 mm diameter), it is wise to form an SF bundle into 200 x 200mm. The de-magnification factor is over 8:1 ($200/25 \times 1.41 = 11.3$). A tapered fiber optics of 4:1 is available and which, with an output relay lens of 3:1, will make a suitable demagnification of 12:1. Thus, an interface of a large-area fiber bundle with a small diameter read-out device can be achieved by using commercially available coupling devices.

4-2 Multi-Anode Photo-Counting Tubes

The final optical read-out can be made very fast using a multiple anode PMT. The multi-anode PMT is position sensitive. Candidates for the use of cosmic ray observing SF calorimeter are Philips XP4702 with 8 x 8 anodes, and Hamamatsu R2487-02 with 18 x

17 anodes. Cross talks among anodes are typically less than 5% for these PMT, and the rise time is 4.8 - 5.6 ns at 1400 - 1250 V. Figures 9a and 9b respectively show Philips and Hamamatsu models.

The block diagram suitable for multi-anode PMT signals is shown in Fig. 10. A test of such a tube was made (by Takasaki et al.) by using green color LED with 1mm diameter upon 40mm surface of the PMT. Relative output of such a test is shown in Fig. 11, where peaks at each location show FWHM of about 6mm.

4-3 Charge-Coupling Device (CCD Camera)

The CCD device is slow in data transfer (10 - 100 Hz), however, it is simpler than the PMT in data handling. Since cosmic ray experiments do not receive very high luminosity, the CCD can work well with a slow speed such as 100 ms per event, provided a certain triggering gate be provided to minimize background triggers.

The best device commercially available can be found in Hamamatsu Particle Track Imaging System. It has two-step microchannel plate for image intensification, a built-in gating circuit, 1/2 - 1/3 relay lens, and a CCD camera. The CCD camera has 767 (H) x 490 (V) pixels, and if needed, can be 1050 (H) x 670 (V). This system allows a gating of 100ns (variable) with delay time of 100ns (fixed). Repetition of the gating power supply is up to 2kHz, which is more than sufficient for most of cosmic ray experiments even with a very low energy triggering. Tables 2 and 3 show detailed characteristics of the system. Shutter operation by using an external trigger pulse is possible with this system. Fig. 12 illustrates an example of such an operation.

4-4 Data Acquisition

The two dimensional CCD image of optical outputs can be stored in a magnetic tape, a magneto-optical disc within a second after being digitized by a FASTBUS or a CCD Digitizer board. The stored data can be easily retrieved for object analysis with a conventional PC/AT or a VAX. The software to process such optical images as those of a calorimeter is ready in the GALAI CUE-2 format, and an access to which is relatively easy for an unskilled operator.

5. Expected Performance of A Calorimeter for High Energy Nuclei and Gamma-Rays

The SF Calorimeter studied in this work seems promising for an application to balloon-borne cosmic ray experiments. The payload in this design weighs about 1.2 tons including a gondola. The read-out/recorders are 2-fold (x- and y-axis) or 4-fold (2x- and 2y-axis), being capable of three-dimensional image analysis of cascade showers. The energy resolution, if neglecting degradation of optical yields due to fabrication errors, should be as good as 16% at 1 GeV, which improves at high energy size as a function of $(\Delta)/E = 16\% / \sqrt{E}$. The resolution at 10 TeV should be, therefore, 0.2%. The finite thickness of the calorimeter may degrade the above resolution of 0.2% for 10 TeV showers. The usable thickness up to the shower maximum may cause an error up to 10% for high energy showers, if the longitudinal profile is not well integrated to the shower maximum. Nevertheless, studies using Monte Carlo cascades with 10 TeV energy shows that statistical fluctuation from event to event can be suitably suppressed by integration of electron numbers for different radii. The present study indicated that the degradation factor of resolution due to the finite thickness was within a factor of five of the expected resolution of 0.2% for 10 TeV showers.

Thus, the SF calorimeter, if assembled as carefully as the present specifications, can be used for gamma-ray measurements in the energy region above 1 GeV, and for cosmic ray nuclei above a few GeV/nucleon energies. The high energy gamma rays and nuclei such as 10 TeV or more can be measured to 1%.

6. Summary

A design study of a scintillation calorimeter for a cosmic ray observation is made. An evaluation of various fibers and design configuration was made. The proposed design has a dimension of 1 m (W) x 1 m (L) x 16 cm (H) contains 1000 fibers at each of 40 x- or 40 y-layers interleaved with 1mm thick leadplates. Two or four CCD Particle Track Imaging Systems are connected to a bundle of SF edges at x- and y-ends. The overall weight of a calorimeter is 1,200 kg including read-out systems and supporting boards. The designed calorimeter can measure cosmic ray nuclei and gamma-rays with position, angles and energy information suitable for detailed spectrum analysis.

The system is particularly beneficial at very high energies where the flux is extremely low and it requires a very long exposure over many years in space. Emulsion chambers have an advantage for cosmic ray measurements if the exposure is limited to several months in space.) In fact, the most important energy region for the current cosmic ray studies is at around 1,000 TeV where a drastic change of elemental composition is indicated by various indirect observations. A detector whose size is in the order of 1 m² requires several years of exposure in space to accumulate sufficient statistics near 1,000 TeV. Emulsions will be strongly contaminated by background radiation for such a long duration flight, while SF calorimeter is totally immune from this concern. This is particularly important for long-duration experiments. The SF calorimeter also allows time-tagging of individual events, extending the experimental capability in various ways.

7. References

1. C. Angelini et al., Nucl. Instr. Methods A295, 299 (1990); A289, 356 (1990); A281, 50 (1989).
2. M.N. Atkinson et al., Nucl. Instr. Methods A263, 333 (1988).
3. P. Destruel et al., Nucl. Instr. Methods A276, 69 (1989).
4. H. Ikeda et al., Nucl. Instr. Methods A292, 439 (1990).
5. F. Takasaki et al., Nucl. Instr. Methods A260, 447 (1987).
6. F. Takasaki, private communication (1990).
7. J. Kirkby, CERN-EP 87-60 (1987).
8. P. Mattern et al., IEEE TRAN NS-21, 81 (1974).
9. A. Spowart et al., Nucl. Instr. Methods 135, 441 (1976); 140, 19 (1977); 150, 159 (1978).
10. C. Auroet et al., Nucl. Instr. Methods 169, 57 (1980).
11. W.R. Binns et al., Nucl. Instr. Methods 216, 475 (1983).
12. Y. Sirois and R. Wigman, Nucl. Instr. Methods A204, 262 (1985).
13. J.W. Epstein et al., Nucl. Instr. Methods A251, 402 (1986).
14. M. Atkinson et al., Nucl. Instr. Methods A254, 500 (1987).
15. J. Timothy and R. Bybee, SPIE Vol. 265, 93 (1985).

γ

HADRON

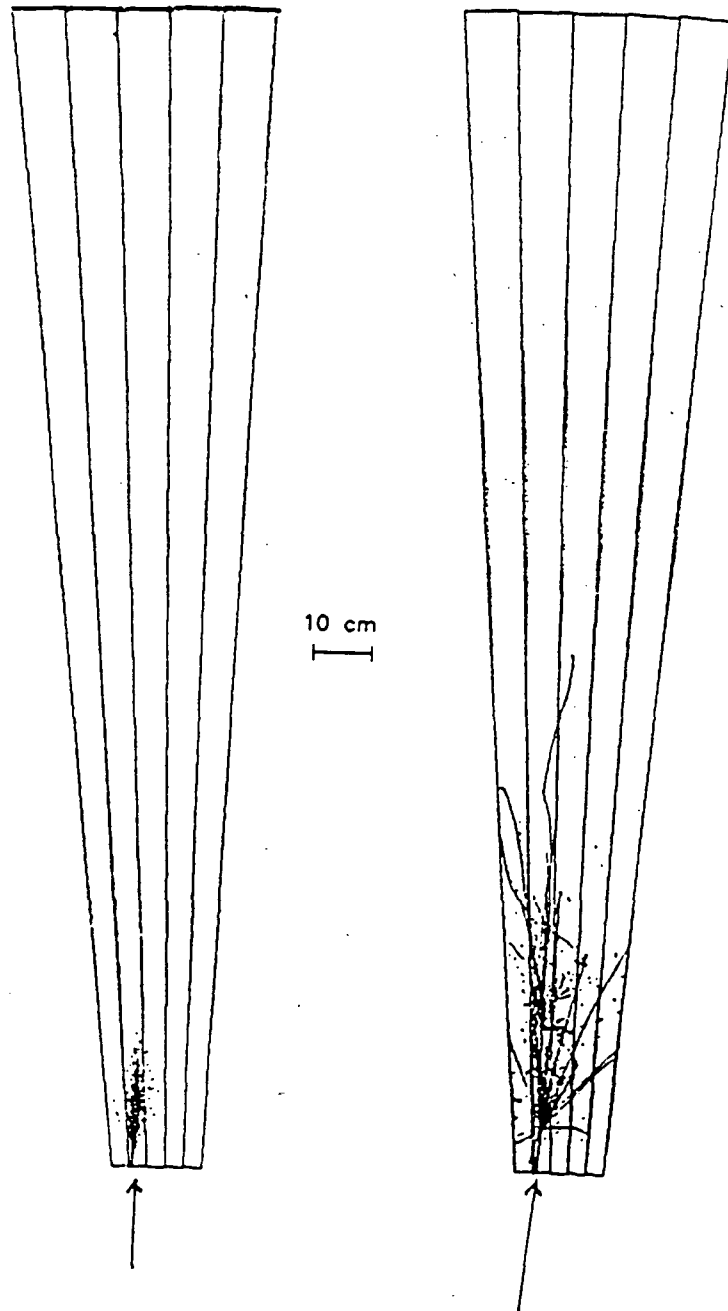
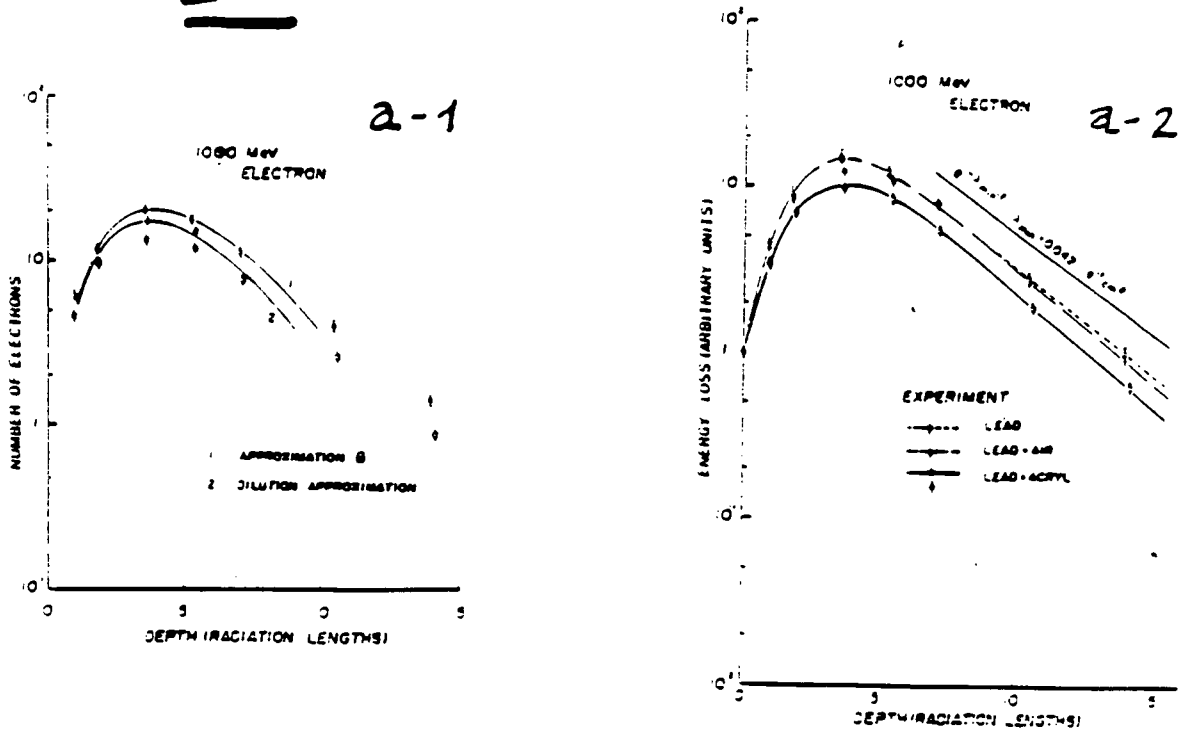


FIG. 1 Difference of lateral developments of showers

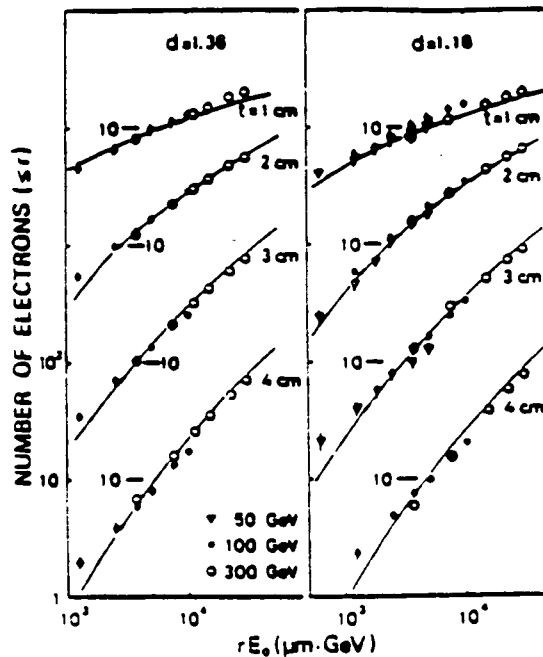
SAMPLING CALORIMETRY

1 D



3 D

b



$$\frac{\gamma E_0}{K} \text{ SCALING}$$

FIG. 1B. Difference in longitudinal development of showers for one-dimensional measurement (a) and that for three-dimensional measurement (b); the latter, giving lateral structure functions at several depths in lead, can be expressed by a similarity law as a function of $r \times E_0/K$ where r and K denote transverse radius and the scattering constant, respectively. (The d is the spacing factor: (lead + space)/(lead) in length.

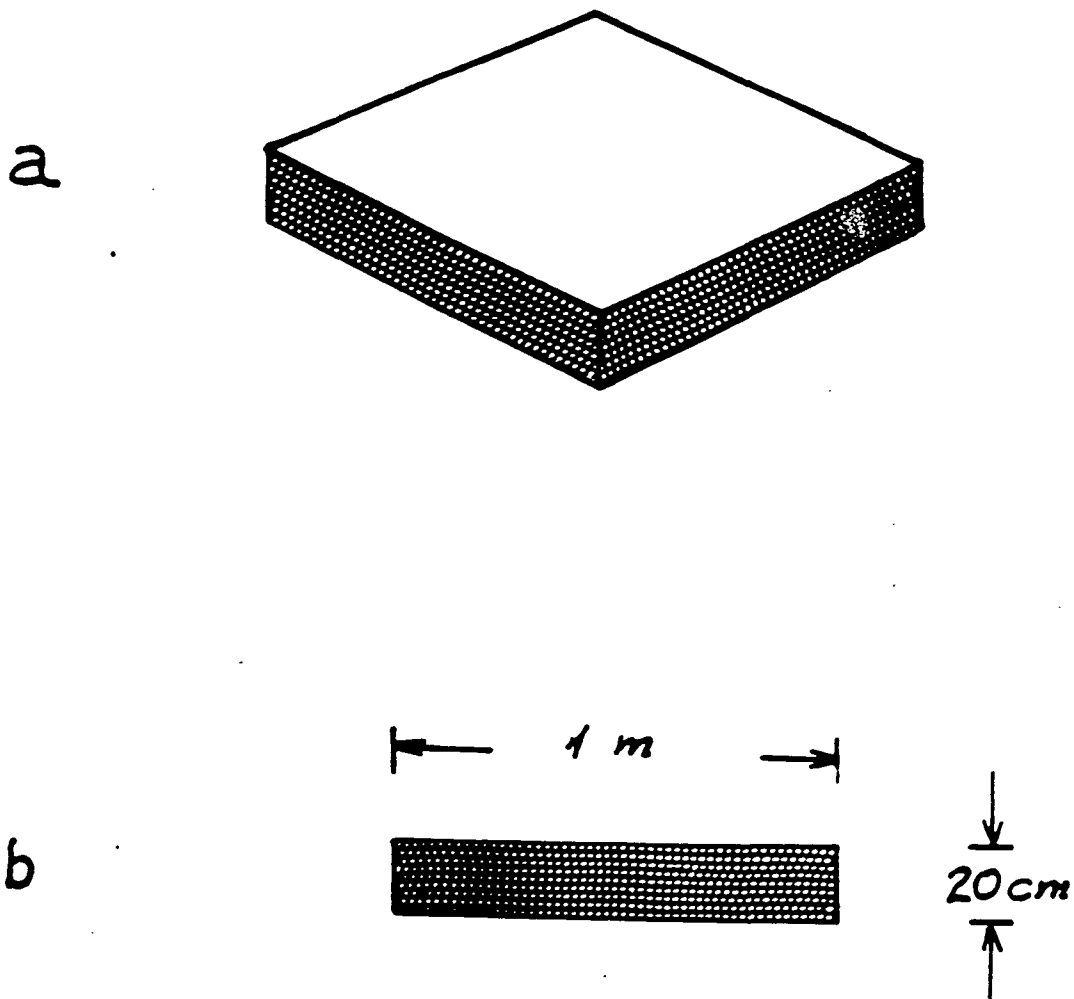


FIG. 2ab. A bird's-eye-view (a) and a side-view (b) of the proposed scintillation-fiber calorimeter.

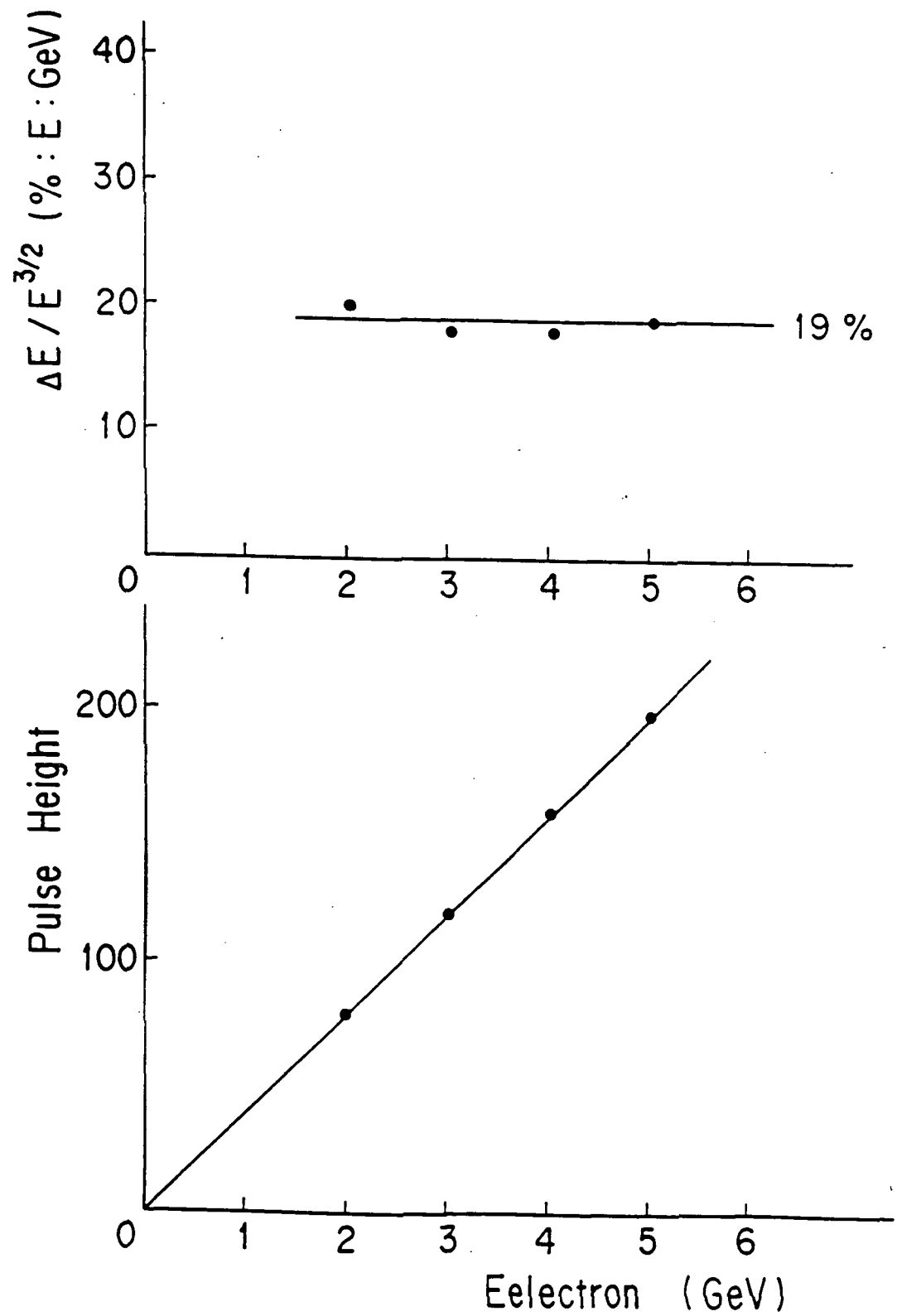


FIG. 3 Energy resolution

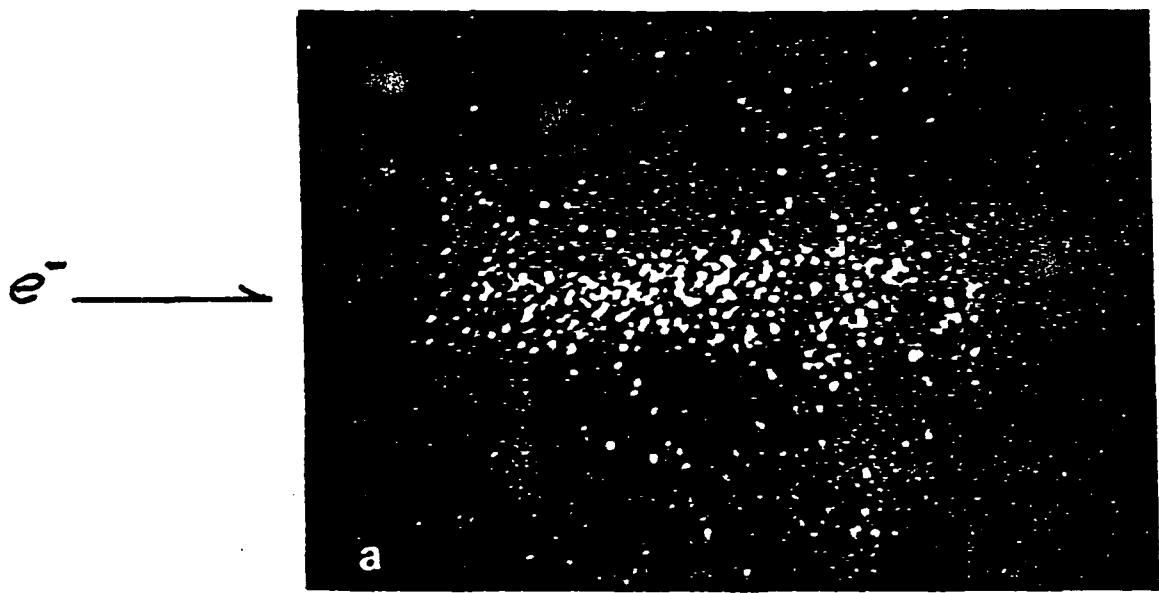
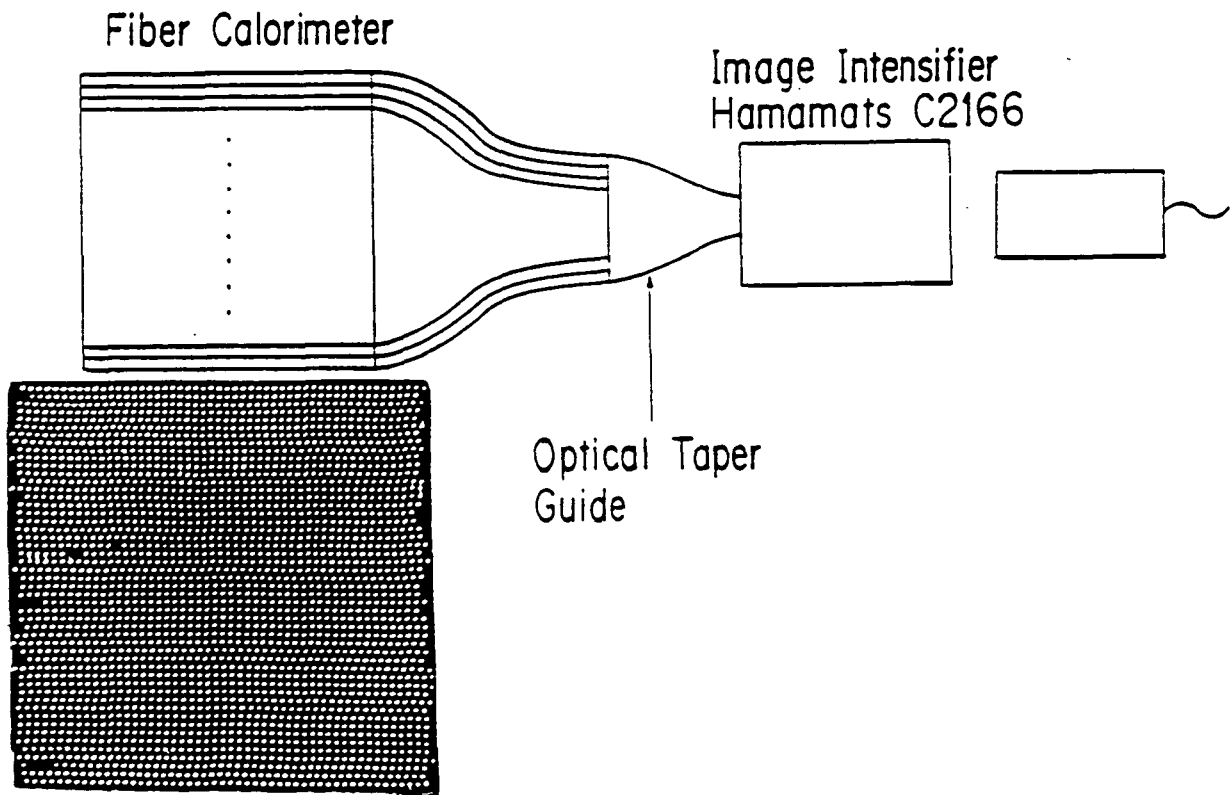


FIG. 4

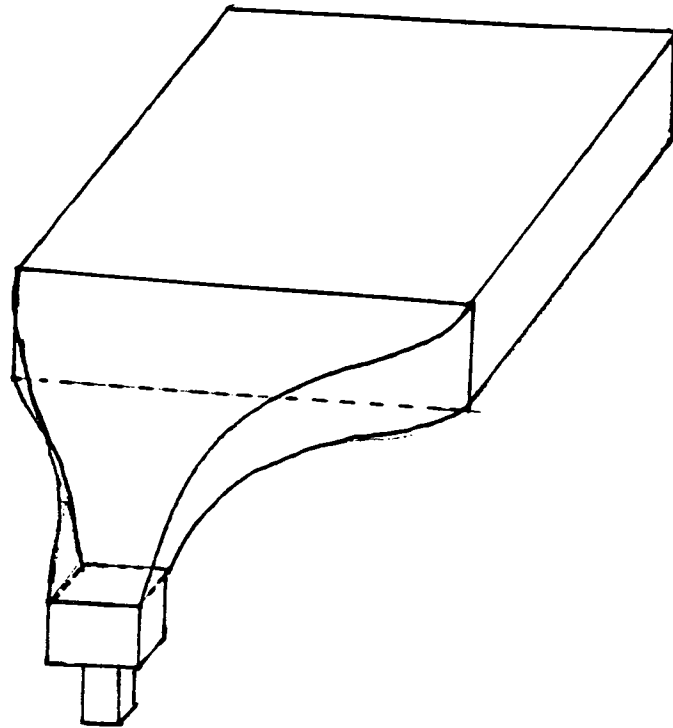


FIG. 5 Schematic illustration of bending of the fiber bundle

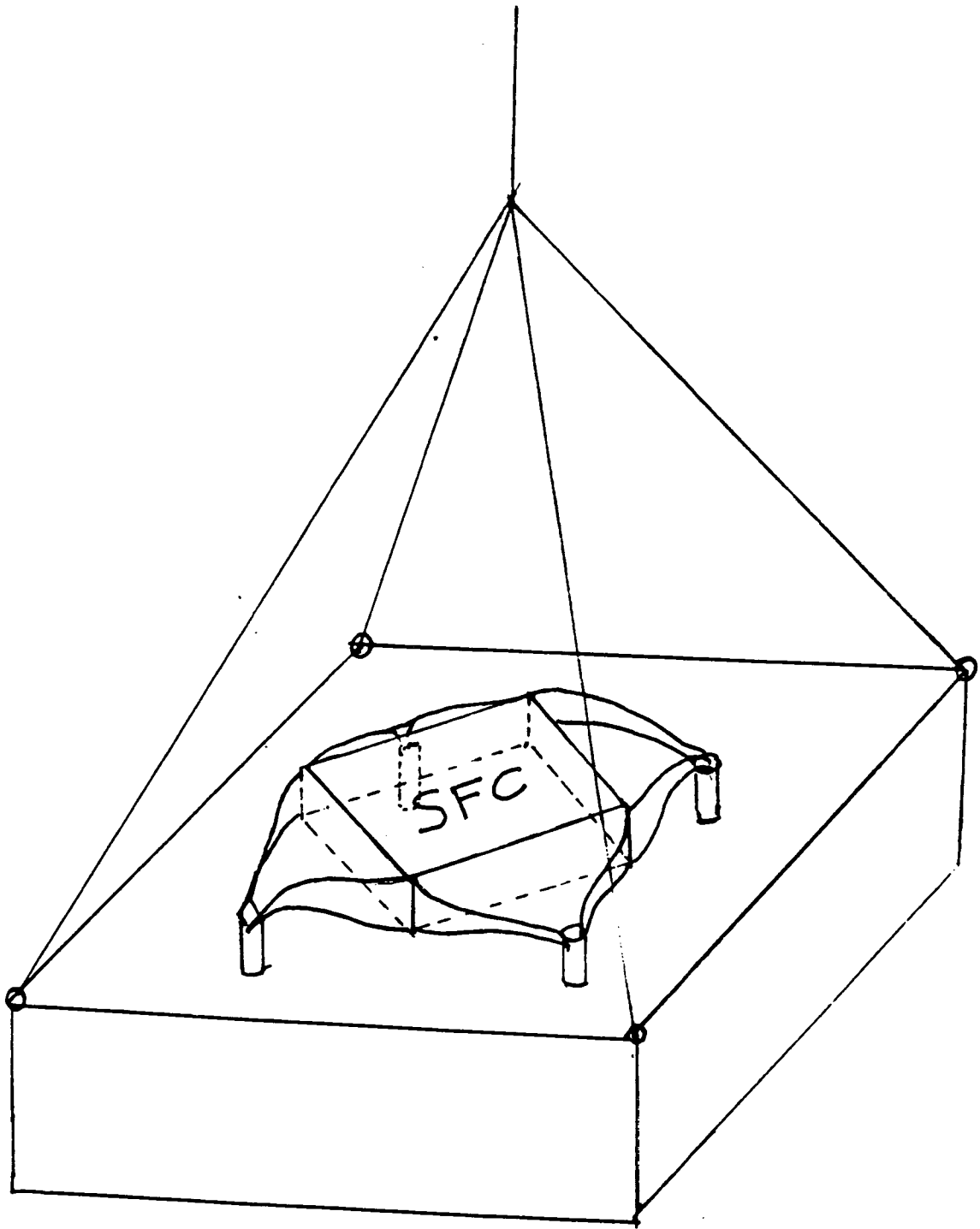
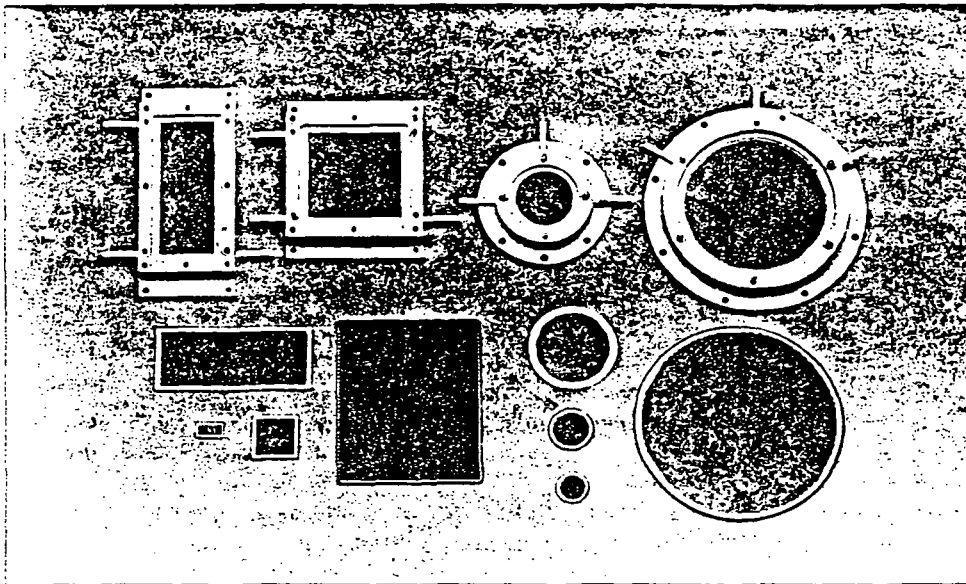


FIG. 6 A gondola concept. Batteries and electronics in the bottom of the box which is made of paper-honeycomb.



A variety of MCP and assemblies

Examples of Products Using MCP

MCP-PMTs

Owing to superior time response and detectivity at low-light levels, MCP-PMTs are useful photodetectors in the fields using lasers. Especially, MCP-PMTs are very effective in time-correlated photon counting which is widely used for biological science and material engineering. (See page 54.) A technical data sheet is available upon request.

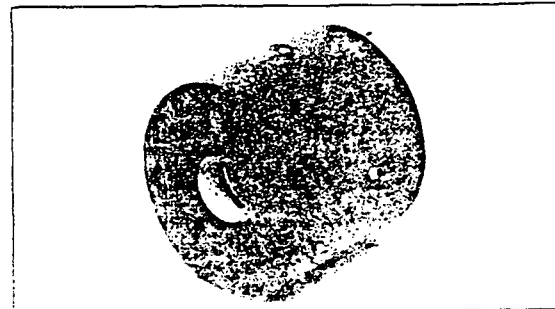


Image Intensifiers

The image intensifier incorporates an MCP which is capable of image intensification of more than 10,000 times. It is widely used in night vision devices, and also its use is spreading to scientific and measurement applications such as astronomical observation, nocturnal animal studies, microscopy, and spectroscopy. A detailed catalog is available from our sales office.



Streak Tubes

The streak tube is an ultra-high-speed photodetector that can capture an ultra-short phenomenon in the order of picoseconds. It provides not only temporal information, but also one-dimensional spatial information. Hamamatsu streak tubes include an MCP which allows high sensitivity.

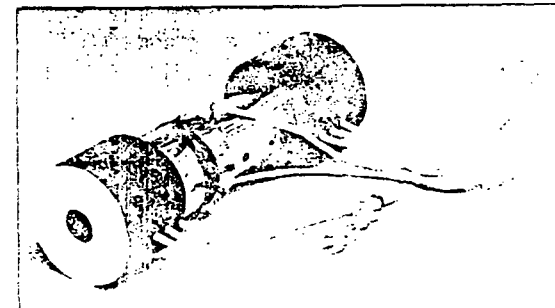


FIG. 7 Micro Channel Plate models

OBJECTIVE SPECIFICATIONS
OF
GATABLE IMAGE INTENSIFIER UNIT

Front Stage II

Spectral Response	370 - 650 nm
Input Window	Fiber Optics
Quantum Efficiency	10% Typ. at 450 nm
Effective Cathode Size	25 mm ϕ
Gain	3×10^3 at 1000V on MCP
Magnification	1.0
Phosphor Screen	P-20
Output Window	Fiber Optics
Effective Screen Size	25 mm :

Later Stage II

Spectral Response	350 - 910 nm
Input Window	Fiber Optics
Quantum Efficiency	10% Typ. at 550 nm
Gain	3×10^3 at 1000V on MCP
Magnification	1.0
Phosphor Screen	P-20
Output Window	Fiber Optics
Effective Screen Size	25 mm ϕ

Unit Dark Counts	100 cps at DC Mode / 25 mm :
Optical Coupling of IIs	Fiber Optics

Power Supply Unit

1) P.S for Front Stage II	Input AC 100V/115V/220V
(C3625)	Adjustable Voltage for MCP
2) Gate P.S. for Later Stage II	Input AC 100V/115V/220V
(C3625-01)	Gate Pulse : TTL / High True
.....	Delay Time : 100 nS
.....	Gate Repetition : 2 KHz Max.
.....	Gate Time : DC-100 nS

Option

Tapered Fiber Optics	4:1 Magnification (Development)
Output Relay Lens	1/2 Magnification LENS
CCD Camera	HAMAMATSU C3057

Unit Construction

1) II Housing with two II's.....	1 pce
2) P.S for Front Stage II	1 pce
3) Gating P.S for Later Stage II	1 pce
4) Cable	1 unit

Table 2 Image Intensifier characteristics

Fig. 8 Optical responses of the image intensifier

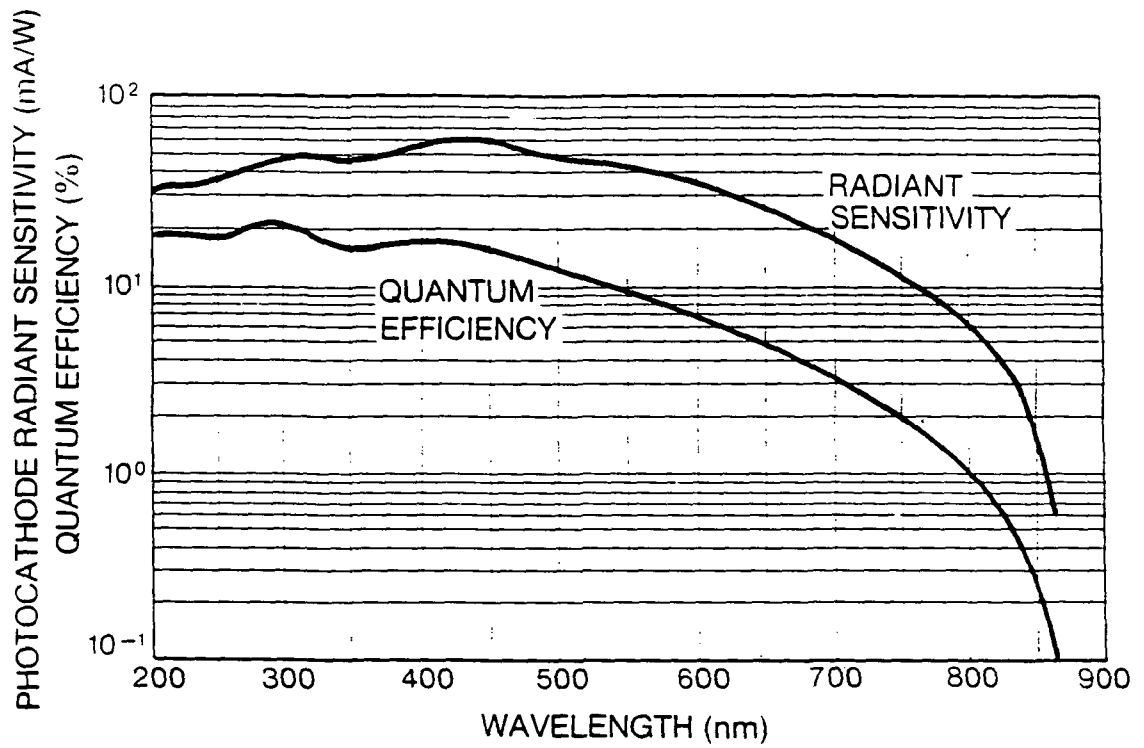


Figure 1: Photocathode Spectral Response Characteristic

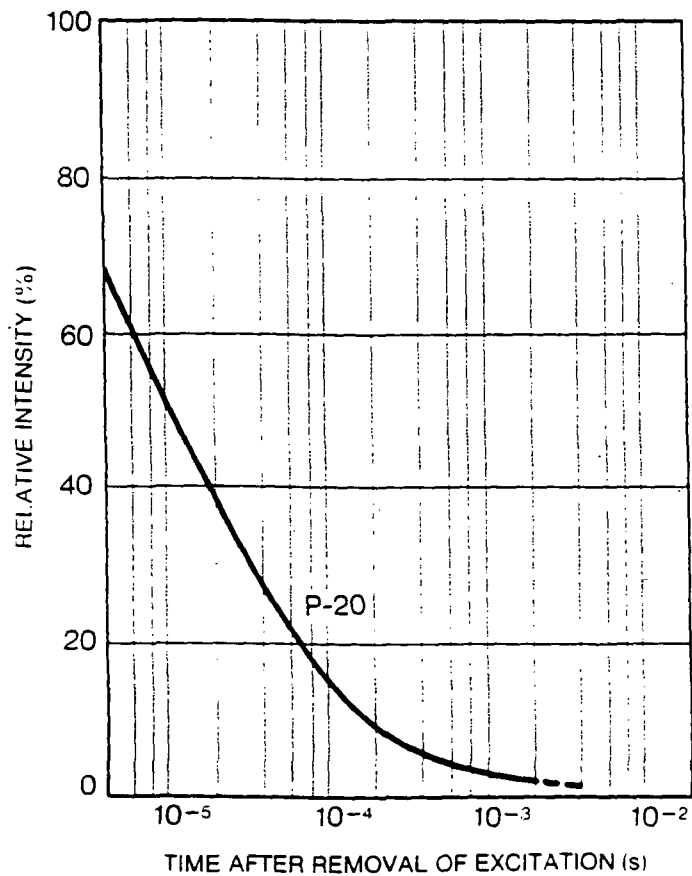
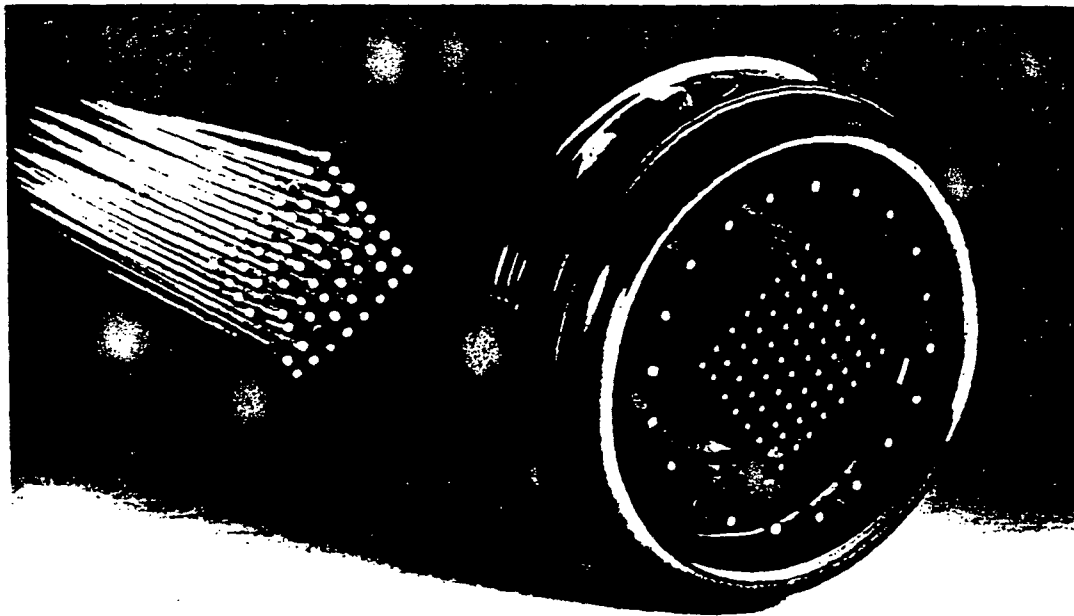


Figure 2: Phosphor Screen After-glow Characteristic



SCINTILLATING FIBRES?

XP4702 reads them out 64 at a time!

First of a new family, the XP4702 extends PMT talents into the realm of spatial as well as time resolution. Combined in a single envelope, 64 ten-stage multipliers with long-life CuBe dynodes produce an 8x8 mosaic of discrete pixels. With uniform channel-to-channel gain and transit-time. The common anode supplies an additional signal that can be used for amplitude analysis or triggering.

Sk _e (λ)	40 mA/W at 400 nm
G	10 ⁶ at 1400 V
t	4.8 ns at 1400 V
output	segmented last dynode, 8x8 matrix of 64 independent 2.54 mm x 2.54 mm elements
crosstalk	< 5% (scanned by 50 μm light spot)

XP4702 opens new opportunities in fibre readout, hodoscopy, calorimetry and coarse imaging. Reference: NIM A269 (1988) 246-260.



Fibres courtesy of Optectron France
 For more information contact: Philips Components,
 Building BAF2, 5600 MD Eindhoven, The Netherlands
 Telex 35000 pntcni/nl (vevo).

STILL SETTING THE STANDARD

Philips Components



PHILIPS

FIG. 9a Philips XP4702 Phototube

Position Sensitive Photomultiplier Tubes

(For further information, a technical data sheet is available.)

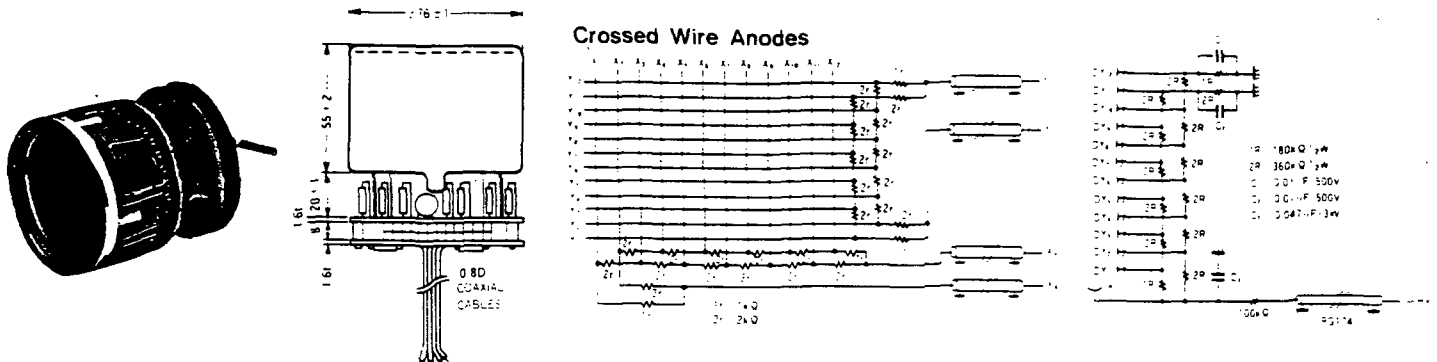
Type No.	Tube Diameter	Spectral Response		Dynode Structure No. of Stages	No. of Anode Wires	Effective Photo-cathode Area Min. (mm)	Maximum Ratings		Cathode Sensitivity		Anode Characteristics			
		Curve Code	Range (nm)				Peak Wavelength (nm)	Anode to Cathode Supply Voltage (Vdc)	Average Anode Current (mA)	Luminous Typ. ($\mu\text{A/lm}$)	Blue ($\mu\text{A/lm-bl}$)	Anode to Cathode Supply Voltage (Vdc)	Anode Sensitivity Radiant Typ. (A/W)	Luminous Typ. (A/lm)

*R2486-02	3" Dia.	403K	300 - 600	420	Mesh	12(X)×12(Y)	40(X)×40(Y)	1300	0.1	60	7.0	1250	6.0×10^{-3}	60	1.0×10^5	20
*R2487-02	3"×3"				12	18(X)×17(Y)	55(X)×45(Y)									

- (A) *: Newly listed in this catalog.
- (B) Typical spectral response characteristics are shown on page 76 and 77.
- (C) The maximum ambient temperature range is -80 to -50°C.
- (D) Average over any interval of 30 seconds maximum.
- (E) At the wavelength of peak response.

Unit: mm

R2486-02



R2487-02

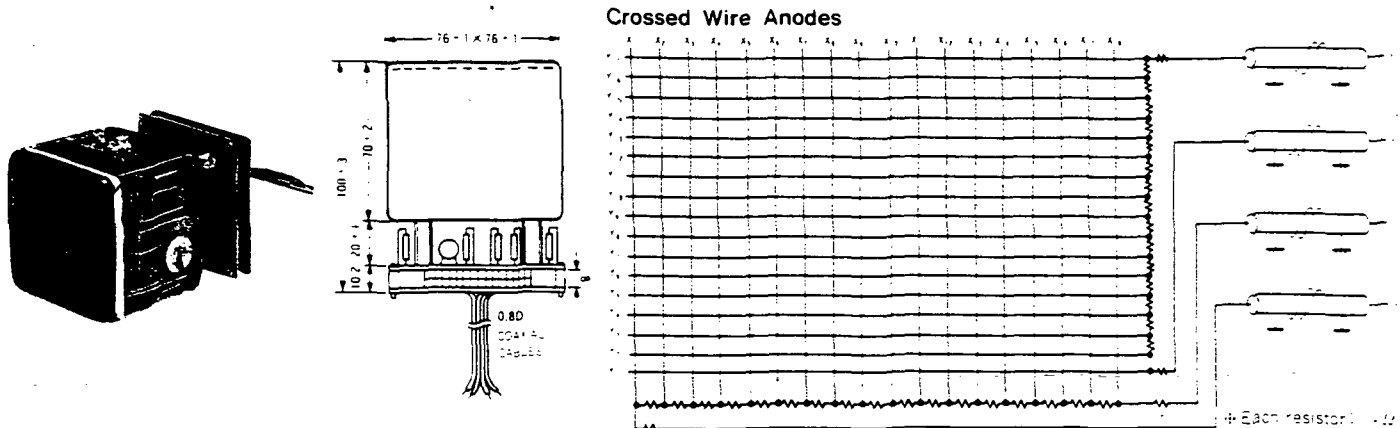
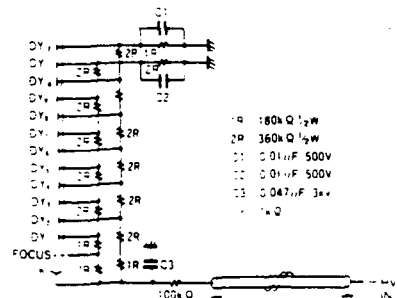


FIG. 9b Hamamatsu R2487-02 Phototube



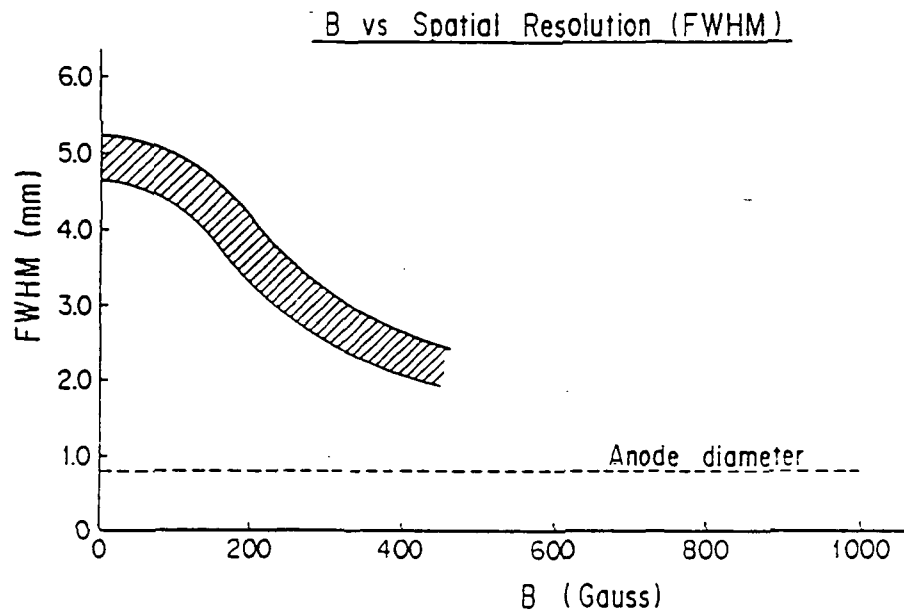
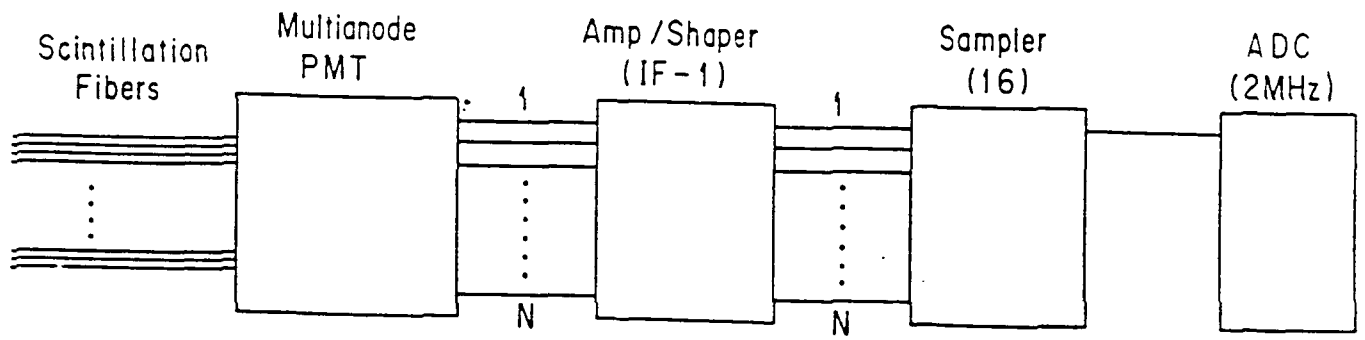


FIG. 10 Signal processing of PMT output, and Spatial Resolution of PMT

FIG. 11 Pulse-height spectra of Multi-anode PMT lead-out calibrated by LED

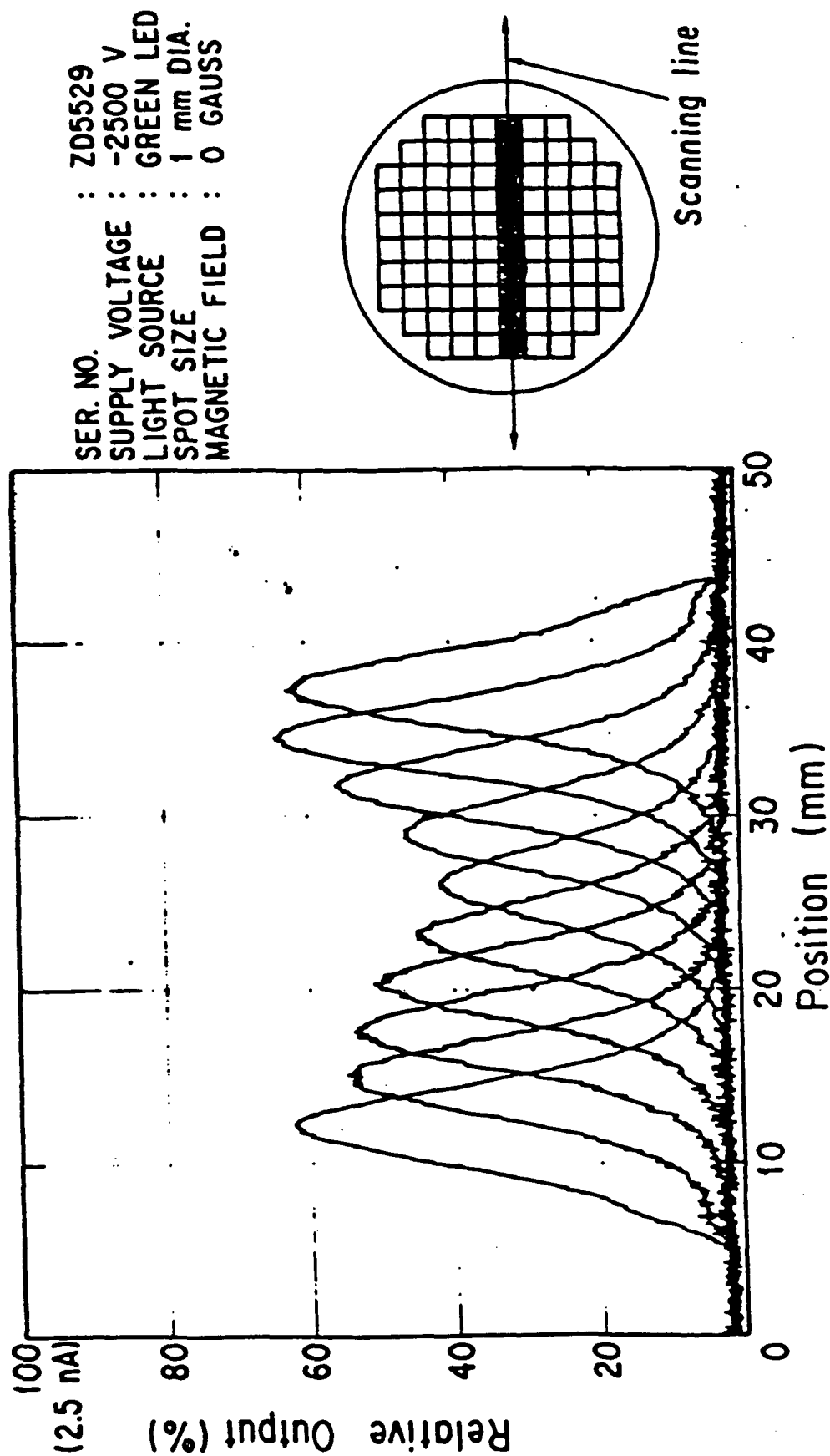


Fig. 3. Pulse-height spectra for LED light scanning along the arrow shown in the attached figure.

CCD Single-unit imaging element section

Transfer method	Frame transfer
Type of image accumulation	Field accumulation (1/60 s)
Number of pixels	767 × 490 (H × V)
Image area	8.8 mm × 6.6 mm
Cell size	11.5 μm × 13.5 μm (H × V)
Minimum photocathode illuminance	4 × 10 ⁻⁵ lux
Type of II/CCD optical composition	1:1 Fiber composition
Resolution limit	350 TV lines
Shutter time	100 ns ~ 14 ms
Shutter repetitions (Input from external trigger)	2 kHz max.
Image distortion	1% max.
Overall γ characteristic	Approx. 1.0 (switchable)
Type of signal	EIA
Scanning frequency	Horizontal frequency 15.734 kHz ± 1%
	Vertical frequency 59.94 Hz ± 1%
Type of scanning	525 lines 2:1 interlace
Image output	1 V _{p-p} , 75 Ω unbalanced

Auxiliary output pulse (AUX) (5 pin connector)

Horizontal drive signal output	HD 4V _{p-p} 75 Ω terminator
Vertical drive signal output	VD 4V _{p-p} 75 Ω terminator
Field index output	F.I 4V _{p-p} 75 Ω terminator
Sample & hold output	S & H clock pulse 14.3 MHz 2V _{p-p} 75 Ω final

Camera Control Unit C3555**Image intensifier gain adjustment control**

Type of control	Manual vernier knob (10-turn, front panel)
-----------------	--

Shutter operation

Shutter operation mode	
Internal trigger mode	Synchronous with internal VD signal
External trigger mode	TTL positive 100 ns min. Shutter delay time 180 ns
	Rear panel BNC connector
Shutter time monitor output	TTL positive 50 Ω terminator
	Rear panel BNC connector

External synchronization

External synchronization through use of HD, VD (Rear panel, BNC connector)	
HD	Pulse height 2 ~ 4 V _{p-p} ; Input impedance 1 kΩ, TTL synchronous negative Pulse width 1 μs min. Frequency 15.734 kHz ± 2%
VD	Pulse height 2 ~ 4 V _{p-p} ; Input impedance 1 kΩ, TTL synchronous negative Pulse width 65 μs min. Frequency 59.94 Hz ± 2%
External synchronization using reset pulse (Rear panel, BNC connector)	
RESET	Pulse height 2 ~ 4 V _{p-p} ; Input impedance 1 kΩ, TTL synchronous negative Pulse width 1 μs min., Frequency 10 Hz max.

Excess incident light protection circuit

Excess incident light detection	Detection of mean value of image signal
Type of control	Control of MCP voltage of II
Display	PROTECT LED flashes when protection circuit is activated Front panel
Protection from excess light outside range of control	Image intensifier shutter off PROTECT LED flashes continuously

General Specifications

Power supply	85 ~ 264 VAC 47 Hz ~ 63 Hz
Power consumption	25 VA
Ambient operating environment	0°C ~ +38°C; Humidity RH 70% max.
Storage temperature	-20°C ~ +50°C

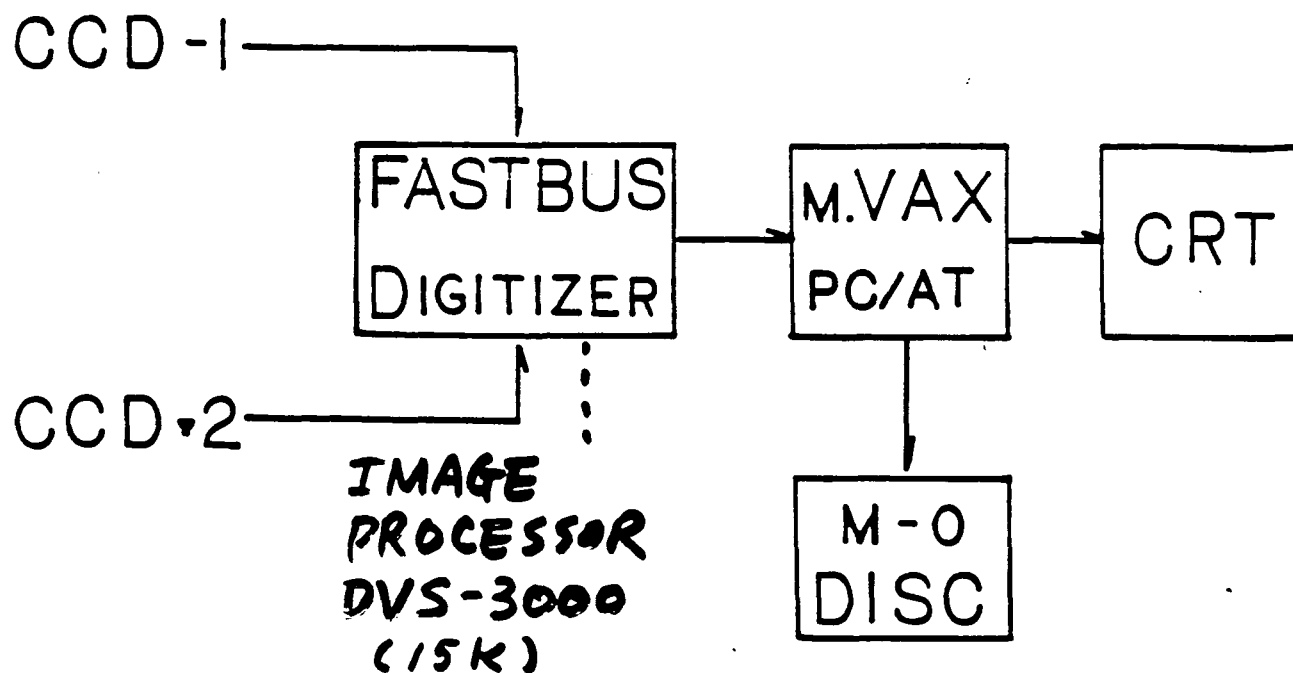


FIG. 12 CCD DATA PROCESSING LAYOUT

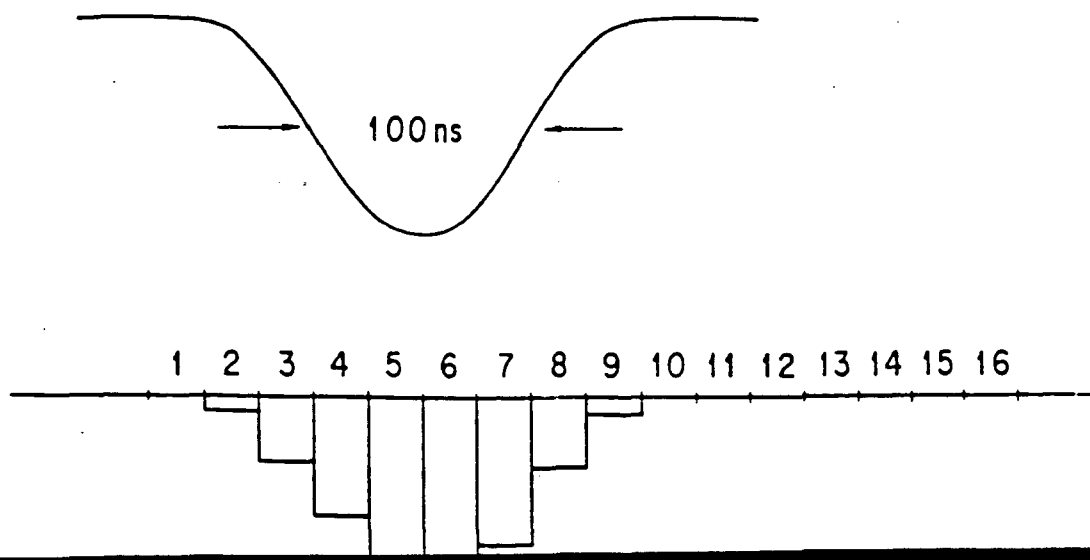


FIG. 12b Gated CCD read-out system (Timing scheme)

ous

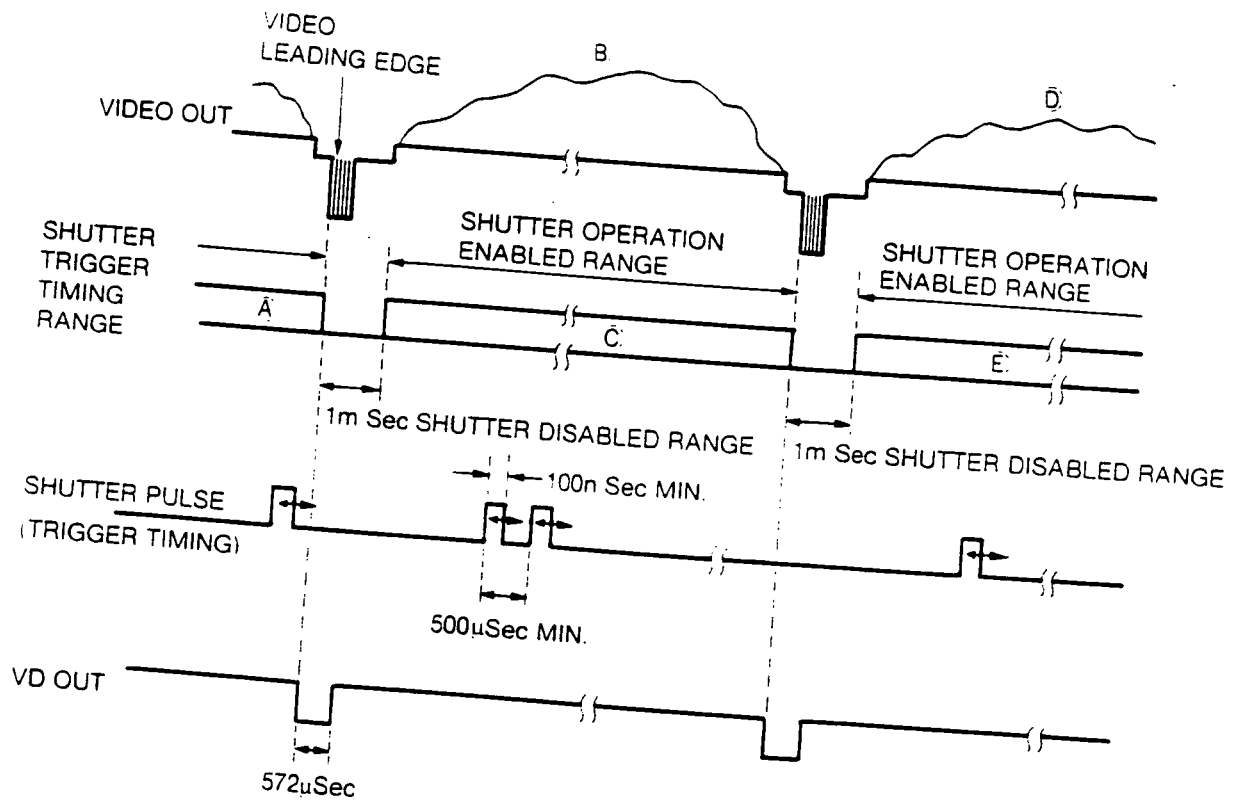


Figure 4: Shutter Operation by External Trigger Pulse

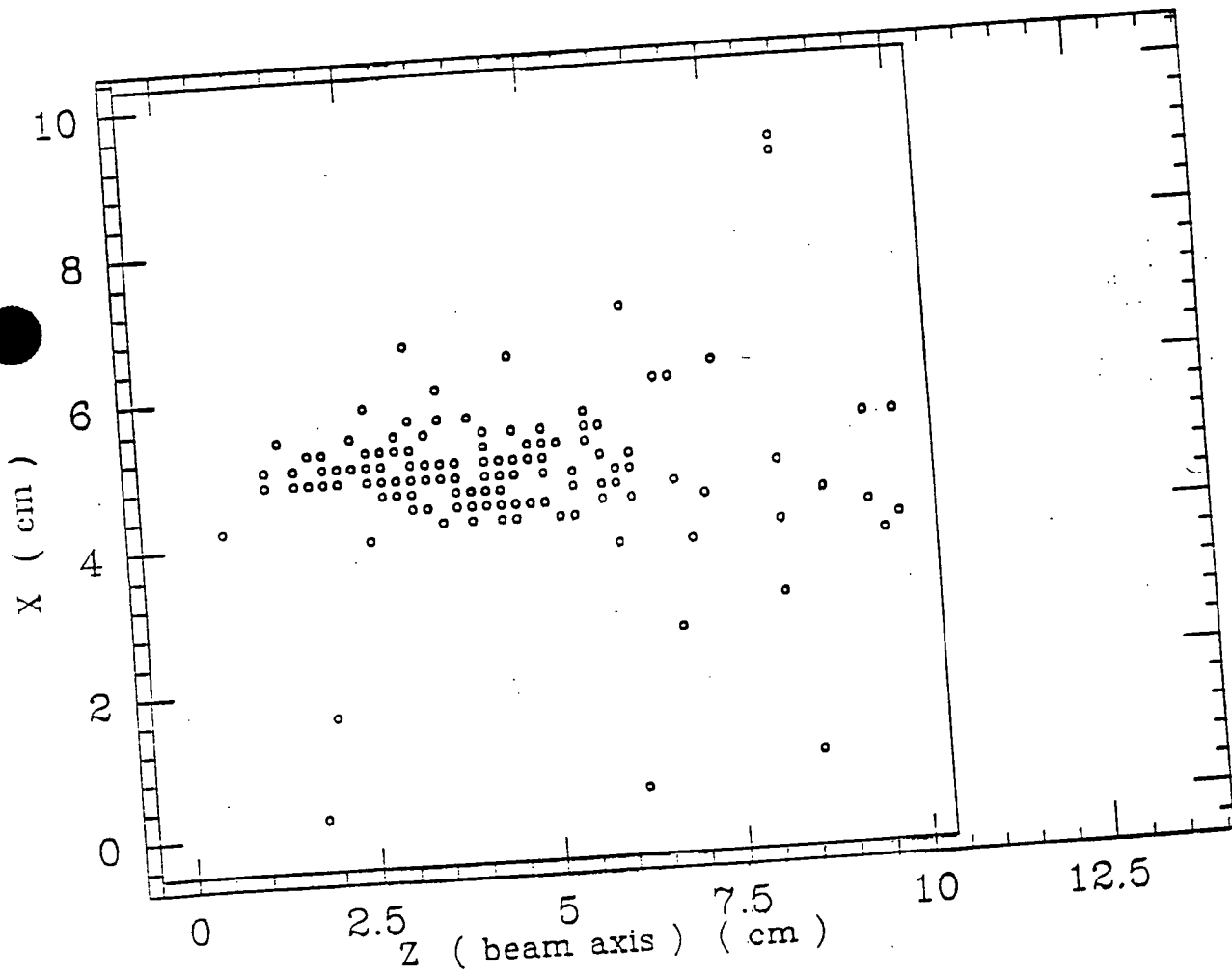


FIG. 13 Digitized CCD read-out